Learning Antenna Pointing Correction in Operations: Efficient Calibration of a Black Box

Leif Bergerhoff
German Aerospace Center (DLR)
German Remote Sensing Data Center (DFD)
National Ground Segment (NBS)
Neustrelitz, Germany
Leif.Bergerhoff@dlr.de

***Abstract*—We propose an efficient offline pointing calibration method for operational antenna systems which does not require any downtime. Our approach minimizes the calibration effort and exploits technical signal information which is typically used for monitoring and control purposes in ground station operations. Using a standard antenna interface and data from an operational satellite contact, we come up with a robust strategy for training data set generation. On top of this, we learn the parameters of a suitable coordinate transform by means of linear regression. In our experiments, we show the usefulness of the method in a real-world setup.**

***Index Terms*—satellite data reception, machine learning, linear regression, coordinate transform, application, operations, homogeneous coordinates, homography**

I. Introduction

An accurate calibration of antenna pointing is crucial for robust and reliable communications between a ground station and satellites. To maximize the received signal strength from the satellite, people came up with various strategies to optimize the orientation of ground station antennas. A traditional method is the so-called step track [1] technique. Extensions and numerous antenna pointing strategies have been suggested (see e.g. [2]–[7] and the references therein). These include applications to stationary [7] as well as mobile systems [4]. Usually, the sun or other cosmic radio sources serve as a reference in order to estimate the desired antenna and environmental parameters. This involves the measurement of offset angles, which, however, often entails an interruption of operations and requires human intervention. Typical parameters include the hardware's mechanical structure, weather conditions, and the target position in the sky [8].

At the ground station Neustrelitz, the German Remote Sensing Data Center operates multiple antenna systems for payload data acquisition from remote-sensing satellites. Satellite communication takes place in different frequency bands: L-, S-, X- and Ka-band, i.e. within a frequency range from 1 GHz to 40 GHz (cf. [9]). One of the antennas [10] is part of the Ionosphere Monitoring and Prediction Center (IMPC) [11] and contributes to the Real Time Solar Wind (RTSW) observation network [12]. Within this context we are engaged in the S-band data reception of the ACE [13] and DSCOVR [14] satellites. Both satellites are positioned at the Sun-Earth L_1 Lagrange point which means that – from a ground station perspective – the trajectories roughly correspond to the position of the sun. As a consequence, our antenna system is used for data reception from sunrise to sunset. From a scientific and practical viewpoint, it is desirable to prevent data loss and antenna unavailabilities in order to be informed about solar events and their potential impact on infrastructure in space and on earth (see e.g. [11]).

A. Our Contributions

We come up with a versatile calibration strategy for semi-automated pointing recalibration of antenna systems. The primary focus of our approach is the applicability in parallel to the operational satellite data reception, i.e. without signal loss. Furthermore, it requires no special knowledge about the construction and the implementation of the antenna system. Our method treats the device as a black box, i.e. a plain antenna with two degrees of freedom and a simple standard interface. We suggest a reasonable coordinate transform for antenna pointing correction and describe the parameter learning using a linear regression approach. In our experiments, we show the applicability to an antenna system in a real-world scenario and prove the usefulness and optimality of our approach. To the best of our knowledge, this is the most comprehensive method considering antenna parameter learning, technical signal information processing, and operational satellite data reception at the same time.

B. Structure of the Paper

In Section II we discuss the basic properties of our black box antenna system and the employed technical signal information. Section III introduces the required coordinate transform and linear regression model.

In Section IV, we develop a calibration strategy and prove their usefulness in experiments.

We conclude with a summary and outlook in Section V.

II. Technical Background

We aim for a software-based calibration procedure which does not need any special knowledge about the implementation of the antenna system. For this purpose, we consider an antenna with two degrees of freedom (azimuth and elevation axes) and a simple interface for tracking information. It

TABLE I
EXCERPT FROM A TYPICAL TRACKING TABLE

Time (UTC)	Azimuth [°]	Elevation [°]
07:18:21	114.67	0.00
07:29:45	116.97	1.53
07:41:09	119.28	3.03

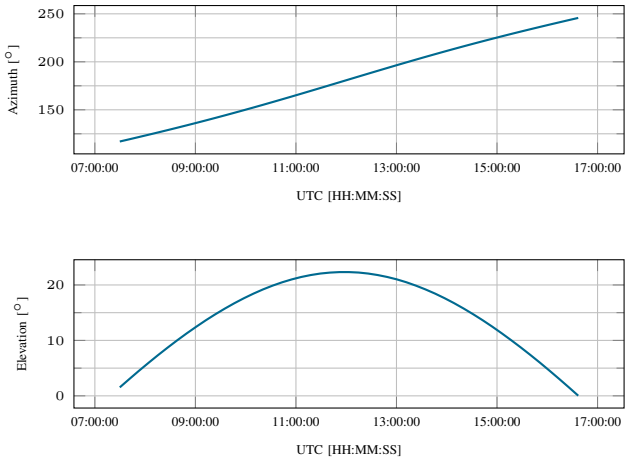

Fig. 1. Exemplary antenna pointing towards the DSCOVR satellite.

permits to upload a tracking table which describes the antenna orientation over time. In our case, this corresponds to the trajectory of the DSCOVR satellite from the antenna's point of view. Table I shows the content of a typical tracking table, containing columns for *time*, *azimuth*, and *elevation* angle. A standard antenna system aligns with the specified tracking points and interpolates the pointing directions in between. Our antenna supports the specification of up to 100 different track points within one file. Fig. 1 visualizes an exemplary antenna pointing for DSCOVR data reception over time.

During operations, the related ground station hardware and software supplies technical signal information. Traditionally, ground station processes use this data for monitoring and control purposes. We store this knowledge and employ a small subset of the data, namely the signal level information, as a measure for the reception quality. Our signal levels are given in dBm (decibel-milliwatts). Given a power P in mW, the corresponding power level x in dBm is calculated as follows:

$$x = 10 \cdot \log_{10} \frac{P}{1\ \text{mW}}\,. \tag{1}$$

In combination with the previously mentioned tracking table, this allows us to draw conclusions about the influence of the antenna pointing on the measured satellite signal strength. In Fig. 2, we illustrate our signal quality assessment process: We use a static tracking table which we upload to the antenna system in advance of the satellite data reception. As mentioned before, the antenna points to the specified directions during operations and interpolates in between. Note, that using this simple – file-based – standard interface it is not possible to change the antenna orientation dynamically. This would

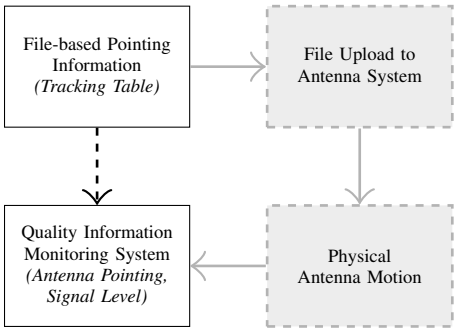

Fig. 2. The basic evaluation process for antenna pointing quality.

require the upload of new pointing information to the system and interrupts the operational satellite communication. In parallel to the satellite data reception, we measure and store the received signal level over time.

III. THEORY AND MODELING

The main task of our antenna pointing calibration method is the estimation of a suitable coordinate transform

$$\boldsymbol{y} := f(\boldsymbol{x}) := \mathbf{T}\boldsymbol{x} \tag{2}$$

for optimal antenna orientation. The coordinate transform f allows to estimate p-dimensional device specific pointing coordinates $\boldsymbol{y} \in \mathbb{R}^p$ from the desired pointing directions $\boldsymbol{x} \in \mathbb{R}^p$. Within this paper, we implement f in terms of a matrix-vector multiplication with a real-valued $p \times p$ transformation matrix $\mathbf{T}$. Furthermore, we make use of homogeneous coordinates (see e.g. [15]) in order of being able to describe occurring nonlinear projective geometry in terms of linear mappings. As an example, we have $p = 3$ and $\boldsymbol{x} = s \cdot (x_1^*, x_2^*, 1)^\mathbf{T}$ with arbitrary scalar $s \neq 0$ for two-dimensional pointing information $(x_1^*, x_2^*)^\mathbf{T}$. For simplicity, we set s to 1. The same transfers to $\boldsymbol{y}$.

In order to train an appropriate coordinate transform f, we consider a multiple linear regression model with multiple outputs (cf. [16]):

$$y_k := f_k(\boldsymbol{x}) := \sum_{j=1}^{p} t_{k,j}\, x_j, \quad \forall k \in \{1, \ldots, p\}, \tag{3}$$

where we consider no bias term since our data is centered.

In order to learn the entries $t_{k,j}$ of $\mathbf{T}$, we do least squares approximation, i.e. we minimize the residual sum of squares

$$\text{RSS}(\mathbf{T}) = \sum_{i=1}^{N} \sum_{k=1}^{p} (\boldsymbol{y}_{i,k} - f_k(\boldsymbol{x}_i))^2 \tag{4}$$

using N pairs $(\boldsymbol{x}_i, \boldsymbol{y}_i)$, i.e. $i = \{1, \ldots, N\}$, as training data.

Subsequently, we restrict ourselves to the scenario $p = 3$, making use of azimuth φ and elevation θ angles as x- and y-

TABLE II
TRAINING ERROR

	MAE [°]	MSE [°]
Azimuth φ *(step track)*	0.023918	0.000772
Elevation θ *(step track)*	0.021072	0.000662
Azimuth φ *(improved calibration)*	0.073698	0.010432
Elevation θ *(improved calibration)*	0.064724	0.011275

coordinates respectively. Accordingly, we write the coordinate transform (2) as

$$\underbrace{\begin{pmatrix}\tilde{\varphi}\\ \tilde{\theta}\\ 1\end{pmatrix}}_{:=\boldsymbol{y}} = \underbrace{\begin{pmatrix}t_{1,1} & t_{1,2} & t_{1,3}\\ t_{2,1} & t_{2,2} & t_{2,3}\\ t_{3,1} & t_{3,2} & t_{3,3}\end{pmatrix}}_{:=\mathbf{T}} \underbrace{\begin{pmatrix}\varphi\\ \theta\\ 1\end{pmatrix}}_{:=\boldsymbol{x}}. \tag{5}$$

Thinking in terms of a sphere surface – with arbitrary radius larger than zero – we have $\varphi \in [0, 2\pi)$ and $\theta \in [-\pi, \pi]$. In terms of cardinal directions, we have $\varphi = 0$ (north), $\varphi = \frac{\pi}{2}$ (east), $\varphi = \pi$ (south), and $\varphi = \frac{3}{2}\pi$ (west). On the other hand, the $\theta = 0$ plane refers to the earth surface and $\theta = \pi$ refers to a pointing straight into the sky. We support negative elevation angles for correction purposes. Typically, antenna systems also support small negative elevation values.

IV. Experiments and Calibration Strategy

A. Step Track

1) Training: In our first experiment, we aim for the estimation of a transformation matrix $\mathbf{T}$ by following a manual step track [1] procedure: We use the electromagnetic radiation of the sun in order to estimate locally optimal azimuth and elevation angles. Meanwhile, the antenna operates in *sun track mode* such that it aligns with the sun (e.g. using track information based on [17]). In our setup, it takes approximately 4 minutes to estimate a locally optimal pointing direction $\boldsymbol{y}$ for a given pointing $\boldsymbol{x}$. Throughout one day, we estimate $N = 60$ pairs $(\boldsymbol{x}, \boldsymbol{y})$ which serve as our training data set. Accordingly, we use the latter to minimize (4) and learn a matrix $\mathbf{T}$. The corresponding training error is given in Table II. The transformation matrix $\mathbf{T}$ reads

$$\mathbf{T} \approx \begin{pmatrix}0.994773 & -0.017231 & 0.022903\\ 0.007398 & 0.992050 & -0.016989\\ 0.000000 & 0.000000 & 1.000000\end{pmatrix} \tag{6}$$

and resembles an affine transform. The key impact factor is a counter-clockwise rotation by $\sim 0.43°$ in the azimuth-elevation plane.

2) Testing: In order to evaluate the quality of the estimated pointing correction, we use the learned coordinate transform to create an adapted tracking table for operational DSCOVR satellite data reception (see Fig. 4). As a consequence of the previously mentioned limit of 100 track points, our experiment's tracking table consists of 6 minute intervals. Therein, we either use the originally provided pointing directions, the adapted *(learned)* pointing directions, or a convex combination of both *(transition intervals)*. A visualization of this selection strategy can be found in the top plot of Fig. 3.

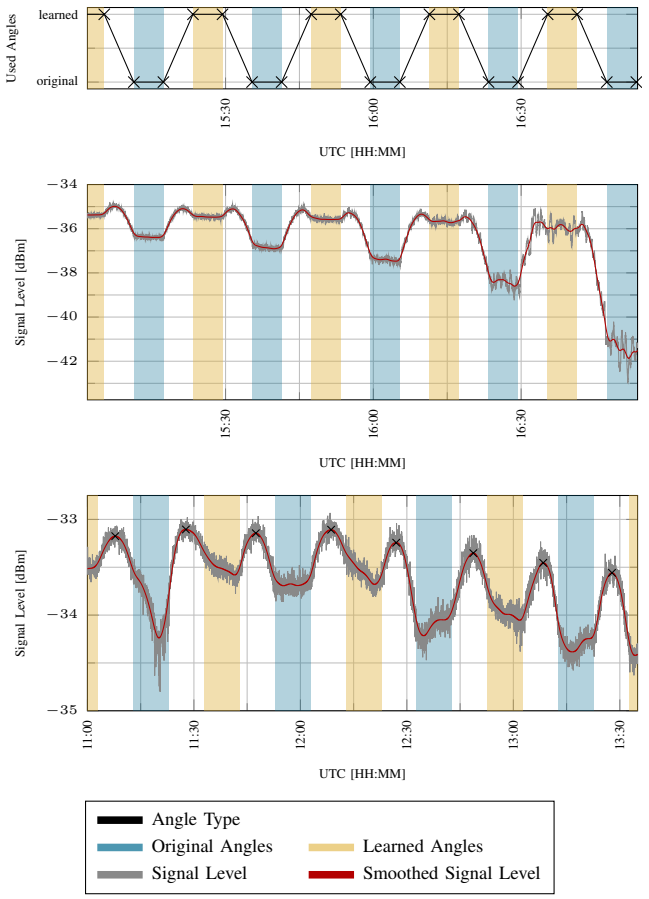

Fig. 3. Pointing direction type and measured signal level. **Top:** Used angle type over time for step track testing. **Middle:** Step track test setup. **Bottom:** Reevaluation of the learned matrix $\mathbf{T}$ and detection of maxima positions.

We illustrate an excerpt of the resulting signal levels in the middle plot of Fig. 3. One can see that there is a gain in signal level of up to 5 dBm (in the afternoon and for low elevation angles). According to (1), this means more than a tripling of the measured signal level. Apart from that, one observes that antenna pointing angles in the transition intervals *(white regions)* lead to slightly higher signal levels in comparison to the learned directions *(yellow regions)*. This indicates that our coordinate transformation is not yet optimal.

Several months later, we repeat the test in order to reevaluate our coordinate transform w.r.t. potentially changed antenna parameters. Due to a longer lasting track and the restriction to 100 points in one tracking table, we have to increase the interval duration to 10 minutes. The bottom plot of Fig. 3 shows that our previous calibration does not lead to significant improvements anymore. Now, better pointing directions clearly lie in the transition intervals. Note that strong signal level changes within the intervals of the original and learned angles (e.g. around 11:20 UTC) can be traced back to obstacles in the signal line of sight.

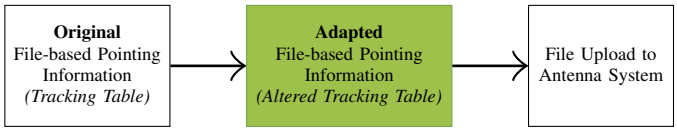

Fig. 4. Process of using our software-based antenna pointing correction.

B. Improved Calibration Strategy

In order to cope with this situation and to prepare for future recalibrations, we come up with a semi-automated calibration strategy. Our procedure is based on the *signal level measurements* which we gain during operations as well as on the *original* and *adapted pointing information* (cf. Fig. 4)). As before, the tracking table contains alternating intervals with original and adapted antenna coordinates. We suggest the subsequent routine for training data set generation:

1) Noise reduction: application of a low-pass filter (e.g. Gaussian filter) to the signal level measurements
2) Estimation of the signal level maxima
   a) Detection of preliminary signal level maxima (e.g. based on negative second derivatives)
   b) Merging of related preliminary maxima (e.g. using mean shift clustering [18] w.r.t. time)
   c) Optimization of the estimated cluster positions using a first-order optimization method like the heavy ball method [19]
   d) Merging of related optimized maxima positions (e.g. using mean shift clustering)

Next, the corresponding intended and actual pointing coordinates at the times of the detected signal level maxima can be used to learn the matrix $\mathbf{T}$ (i.e. the minimization of (4)).

C. Improved Calibration

1) Training: Now, we can directly apply the suggested calibration strategy to the reevaluation test data (see bottom plot in Fig. 3). We are able to detect $N = 42$ signal level maxima (illustrated as crosses). Accordingly, we use the related original and adapted pointing information to train the new transformation matrix

$$\mathbf{T} \approx \begin{pmatrix} 0.997936 & -0.005520 & 0.007442 \\ 0.002914 & 0.995512 & -0.005053 \\ 0.000000 & 0.000000 & 1.000000 \end{pmatrix}. \tag{7}$$

The corresponding training error is also listed in Tab. II. It is slightly higher than for our manual step track calibration, for reasons visible in Fig. 5. Therein, we depict the estimated as well as the learned azimuth and elevation offsets throughout the satellite data reception. One can observe two outliers with significant impact on the error values: in the azimuth offset at around 10:50 UTC and in the elevation offset at around 17:23 UTC. While the first outlier results from a signal level change induced by the satellite, the second can be traced back to low elevation values and obstacles close to the ground. Overall, the learning has a denoising and stabilizing effect on the offset estimation. This is desirable and limits the impact of the outliers. Again, the matrix $\mathbf{T}$ implements an affine

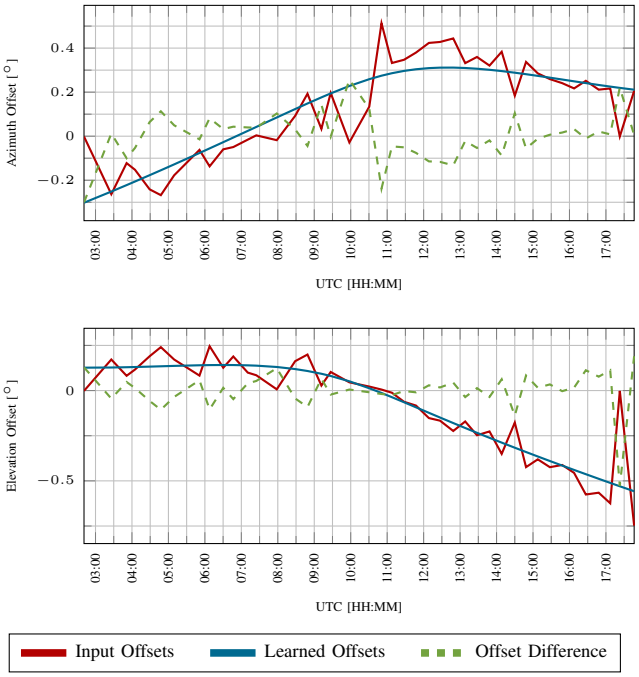

Fig. 5. Estimated and learned offsets using the improved calibration strategy. **Top:** Azimuth angle offsets. **Bottom:** Elevation angle offsets.

transform in the azimuth-elevation plane, i.e.

$$\begin{pmatrix} \tilde{\varphi} \\ \tilde{\theta} \end{pmatrix} = \underbrace{\begin{pmatrix} 0.997936 & -0.005520 \\ 0.002914 & 0.995512 \end{pmatrix}}_{=:\mathbf{A}} \begin{pmatrix} \varphi \\ \theta \end{pmatrix} + \underbrace{\begin{pmatrix} 0.007442 \\ -0.005053 \end{pmatrix}}_{=:\boldsymbol{t}}, \tag{8}$$

where $\boldsymbol{t}$ denotes a translation. The matrix $\mathbf{A}$ describes – in this order – a scaling $\mathbf{S_1}$, a shearing $\mathbf{S_2}$, and a counter-clockwise rotation $\mathbf{R}$

$$\mathbf{S_1} = \begin{pmatrix} 0.997940 & 0.000000 \\ 0.000000 & 0.995524 \end{pmatrix} \tag{9}$$

$$\mathbf{S_2} = \begin{pmatrix} 1.000000 & -0.002625 \\ 0.000000 & 1.000000 \end{pmatrix} \tag{10}$$

$$\mathbf{R} = \begin{pmatrix} 0.999996 & -0.002920 \\ 0.002920 & 0.999996 \end{pmatrix} \tag{11}$$

in the azimuth elevation plane, s.t. $\mathbf{A} := \mathbf{R}\mathbf{S_2}\mathbf{S_1}$. This time, the key impact factor is a counter-clockwise rotation by $0.167279°$.

2) Testing: Subsequently, we demonstrate that the learned antenna pointing correction is optimal and works well in practice. For doing so, we create another tracking table for operational data reception of the DSCOVR satellite. It implements the learned pointing directions as well as an offset strategy which we apply on top. We show the idea of setting azimuth and elevation angle offsets in Fig. 6. The center denotes the previously learned antenna pointing direction. In our test, we deviate from the latter in a cyclic manner. Our cycle consists of 17 sequential track points. Starting with index 0 every second point implements the learned pointing direction (no offset). In all points with uneven index, the pointing directions deviate by $r = 0.75°$. This value is chosen in accordance with the beamwidth of the antenna to prevent a loss of signal. The offset direction – in terms of the azimuth-elevation plane – changes by $\alpha = 45°$ between the track points

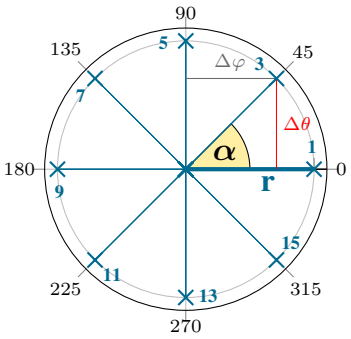

Fig. 6. Offset strategy for the optimality test with track point indices in blue.

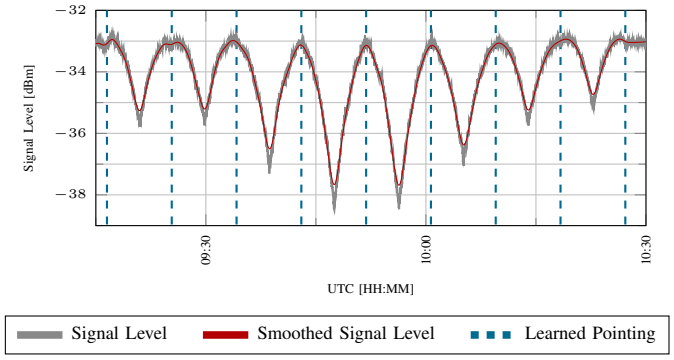

Fig. 7. Measured signal level for one offset cycle in our optimality test.

which implement an offset. In this way, we finish a complete offset cycle after 17 track points. As before, the antenna implements a linear interpolation between all tracking points. One can see the corresponding signal level measurements for one such test cycle in Fig. 7. It is important to note, that the highest signal level occurs very close to the learned antenna pointing (i.e. for track points with no offset). In terms of the local maximum signal level, the mean absolute error for the learned pointing directions is 0.085124 dBm, the maximum error is 0.360258 dBm. We estimate these errors using a minimally smoothed signal level (employing a Gaussian filter with $\sigma = 5$ for smoothing). From our point of view, these errors are negligible, especially due to noise and environmental effects like obstacles on the signal level measurements.

V. Summary and Outlook

In our paper, we have shown an efficient method for antenna pointing recalibration in an operational environment. The proposed calibration strategy implements a robust selection process for training data which is used to estimate a suitable coordinate transform. Within our context, a setup involving a linear transformation is appropriate. In principle, our approach can easily be adapted to support different coordinate transformations. From a practical point of view, the usage of signal level measurements – which are a byproduct of the operational satellite data reception – is a welcome feature. It reduces the need for additional hardware and work steps for antenna pointing calibration. In our future work, we investigate the application of our method to other antenna systems. Amongst others, this requires the consideration of a higher number of degrees of freedom. Furthermore, we want to evaluate the necessity of more comprehensive coordinate transformations w.r.t. different possible sources of antenna pointing errors.

Acknowledgment

I thank my colleagues at the German Remote Sensing Data Center for valuable comments, fruitful discussions, and technical assistance.

References

[1] R. B. Dybdal, "Step tracking performance and issues," in *IEEE Antennas and Propagation Society International Symposium*. IEEE, Jun. 1998, pp. 58–61.

[2] K. G. Holleboom, "Self-learning step track system to point an antenna at a geostationary satellite using a pc," *IEEE Transactions on Consumer Electronics*, vol. CE-33, no. 3, pp. 481–487, Aug. 1987.

[3] K. Dai, S. Zhao, Q. Li, and Z. You, "Research on the automatic calibration of antenna for vehicle telemetry receivers based on solar radiation," in *13th IEEE International Conference on Control & Automation*. IEEE, Jul. 2017, pp. 1084–1089.

[4] Z. Li, X. Yang, and F. Tan, "A novel pointing algorithm for vehicle satellites' antenna," in *2010 IEEE International Conference on Progress in Informatics and Computing*. IEEE, Dec. 2010, pp. 1143–1146.

[5] A. A. Mulla and P. N. Vasambekar, "Overview on the development and applications of antenna control systems," *Annual Reviews in Control*, vol. 41, pp. 47–57, Apr. 2016.

[6] J. Baars, "The measurement of large antennas with cosmic radio sources," *IEEE Transactions on Antennas and Propagation*, vol. 21, no. 4, pp. 461–474, Jul. 1973.

[7] M. Meeks, J. Ball, and A. Hull, "The pointing calibration of the haystack antenna," *IEEE Transactions on Antennas and Propagation*, vol. 16, no. 6, pp. 746–751, Nov. 1968.

[8] B. Nyheim, S. Riemer-Sørensen, R. Parra, and C. Cicone, "Machine learning based pointing models for radio/sub-millimeter telescopes," *CoRR*, vol. abs/2402.08589, Feb. 2024.

[9] "IEEE standard letter designations for radar-frequency bands," *IEEE Std 521-2019 (Revision of IEEE Std 521-2002)*, pp. 1–15, 2020.

[10] T. Siebolds, "Series WTW-LS 42 parabol," http://www.tracking-antenna.de/wp-content/uploads/2015/05/Datasheet_WTW-LS_42_Parabol.pdf, Apr. 2019, last visited 23 February 2024.

[11] M. Kriegel and J. Berdermann, "Ionosphere monitoring and prediction center," in *European Navigation Conference*. IEEE, Nov. 2020, pp. 1–10.

[12] National Oceanic and Atmospheric Administration, "Real time solar wind — noaa / nws space weather prediction center," https://www.swpc.noaa.gov/products/real-time-solar-wind, last visited 23 February 2024.

[13] E. C. Stone, A. M. Frandsen, R. A. Mewaldt, E. R. Christian, D. Margolies, J. F. Ormes, and F. Snow, "The advanced composition explorer," *Space Science Reviews*, vol. 86, pp. 1–22, Jul. 1998.

[14] J. Burt and B. Smith, "Deep space climate observatory: The DSCOVR mission," in *2012 IEEE Aerospace Conference*. IEEE, Apr. 2012, pp. 1–13.

[15] R. Hartley and A. Zisserman, "Scene planes and homographies," in *Multiple View Geometry in Computer Vision*, 2nd ed. Cambridge: Cambridge University Press, 2004, ch. 13, pp. 325–343.

[16] T. Hastie, R. Tibshirani, and J. H. Friedman, *The Elements of Statistical Learning: Data Mining, Inference, and Prediction, 2nd Edition*, 2nd ed., ser. Springer Series in Statistics. New York: Springer, Feb. 2009.

[17] R. S. Park, W. M. Folkner, J. G. Williams, and D. H. Boggs, "The jpl planetary and lunar ephemerides de440 and de441," *The Astronomical Journal*, vol. 161, no. 3, p. 105, Feb. 2021.

[18] Y. Cheng, "Mean shift, mode seeking, and clustering," *IEEE Transactions on Pattern Analysis and Machine Intelligence*, vol. 17, no. 8, pp. 790–799, Aug. 1995.

[19] B. T. Polyak, *Introduction to Optimization*. New York: Optimization Software, 1987.